Analytical and Bioanalytical Chemistry (2021) 413:5949–5967
https://doi.org/10.1007/s00216-021-03490-6

REVIEW

A review of biosensors for the detection of B-type natriuretic peptide as an important cardiovascular biomarker

Meysam Gachpazan[1] · Arash Mohammadinejad[2] · Amin Saeidinia[3,4] · Hamid Reza Rahimi[5] · Majid Ghayour-Mobarhan[6] · Farveh Vakilian[7] · Majid Rezayi[2,6,8]

Received: 15 April 2021 / Revised: 31 May 2021 / Accepted: 17 June 2021 / Published online: 16 August 2021

Abstract

Heart disease, as the most serious threat to human health globally, is responsible for rising mortality rates, largely due to lifestyle and diet. Unfortunately, the main problem for patients at high risk of heart disease is the validation of prognostic tests. To this end, the detection of cardiovascular biomarkers has been employed to obtain pathological and physiological information in order to improve prognosis and early-stage diagnosis of chronic heart failure. Short-term changes in B-type natriuretic peptide are known as a standard and important biomarker for diagnosis of heart failure. The most important problem for detection is low concentration and short half-life in the blood. The normal concentration of BNP in blood is less than 7 nM (25 pg/mL), which increases significantly to more than 80 pg/mL. Therefore, the development of new biosensors with better sensitivity, detection limit, and dynamic range than current commercial kits is urgently needed. This review classifies the biosensors designed for detection of BNP into electrochemical, optical, microfluidic, and lateral-flow immunoassay techniques. The review clearly demonstrates that a variety of immunoassay, aptasensor, enzymatic and catalytic nanomaterials, and fluorophores have been successfully employed for detection of BNP at low attomolar ranges.

Keywords Biosensor · Biomarker · B-type natriuretic peptide · Heart failure

Introduction

Cardiovascular disease is the leading cause of death worldwide, accounting for 31% of all deaths in 2016 globally. In low- and middle-income countries (LMICs), nearly 80% of deaths are related to cardiovascular disease (CVD) [1]. The World Health Organization (WHO) recommends reducing the risk of heart disease through early prevention [2]. Effective prognostic testing is one of the main problems in patients at high risk for heart disease [3, 4]. Although biomarkers have played an important role in the diagnosis of CVD in recent years [5], there is a lack of effective tests for heart failure (HF) prognosis, and the number of these patients is increasing worldwide [6].

Meysam Gachpazan and Arash Mohammadinejad contributed equally to this work.

✉ Majid Rezayi
Rezaeimj@mums.ac.ir

[1] Medical Genetics Research Centre, Faculty of Medicine, Mashhad University of Medical Sciences, Mashhad 9177948564, Iran

[2] Department of Medical Biotechnology and Nanotechnology, School of Medicine, Mashhad University of Medical Sciences, Mashhad 9177948564, Iran

[3] Pediatric Department, Faculty of Medicine, Mashhad University of Medical Sciences, Mashhad 9177948564, Iran

[4] Pharmaceutical Research Center, Mashhad University of Medical Sciences, Mashhad 9196773117, Iran

[5] Vascular and Endovascular Surgery Research Center, Alavi Hospital, Mashhad University of Medical Sciences, Mashhad 9177899191, Iran

[6] Metabolic Syndrome Research Center, School of Medicine, Mashhad University of Medical Sciences, Mashhad 9177948564, Iran

[7] Clinical Research Unit, Faculty of Medicine, Mashhad University of Medical Sciences, Mashhad 9176699199, Iran

[8] Medical Toxicology Research Center, Mashhad University of Medical Sciences, Mashhad 9177948564, Iran

In both types of HF, i.e. HF with reduced ejection fraction (HFrEF) and HF with preserved ejection fraction (HFpEF), left ventricular function is normal in patients [7]. Classification of HF is performed using the American College of Cardiology/American Heart Association (ACC/AHA) and New York Heart Association (NYHA) classification systems. These approaches focus on the importance of structural heart disease or symptoms/absence of symptoms based on physical activities in individuals with HF [8]. Physical examinations are another means for assessing the presence and severity of HF, including the measurement of vital signs in standing and sitting positions [8]. Chest radiography is a routine assessment in patients with HF symptoms and has great potential in situations of vague clinical observation [9], while electrocardiography (ECG) is a standard method for assessment of patients with primary HF [10]. Laboratory panel tests for HF patients include the measurement of blood urea nitrogen, thyroid-stimulating hormone, uric acid, serum creatinine, complete blood count, hepatic enzymes, fasting lipid profile, impregnating transferrin, and urinalysis. In this case, natriuretic peptides (NPs) have many advantages for diagnosis and prognosis that will be described [11].

As HF is a complex clinical syndrome, several factors play an important role in either or both the cardiac myocytes and the cardiac interstitium, such as cardiac overload and complex genetic, neurohormonal, inflammatory, and biochemical variations [12]. These disrupt the filling of the ventricles or the outflow of the blood. In this regard, multiple biomarkers have been applied in evaluating HF patients, including B-type natriuretic peptide (BNP)/N-terminal pro–B-type natriuretic peptide (NT-proBNP), mid-regional pro-adrenomedullin (MR-proADM), and ST2 in myocyte stress or C-reactive protein and tumor necrosis factor in inflammation [12]. The main processes in HF should be reflected by biomarker detection using highly accurate, sensitive, and facile analytical methods [13]. Biomarkers can provide beneficial information about clinical manifestations, rapid detection, prognosis, and successful therapeutic strategies. The most common biomarkers in HF are members of the NP family, which play an important role in the diagnosis, prognosis, and treatment of HF patients [13].

The NP family, including atrial natriuretic peptide (ANP), BNP, and C-type natriuretic peptide (CNP) [14], are involved in regulating blood pressure and hemostasis [15, 16]. NPs are produced to prevent fibrosis and attenuate activation of the renin-angiotensin-aldosterone system (RAAS), and to promote natriuresis and vasodilation. All of these make NPs unique in the maintenance of the cardiorenal system through cGMP activity [17–19]. Among the NP family, BNP and its cleaved form, NT-proBNP, have gained considerable attention for their prognostic utility in coronary heart disease (CHD), and are often measured in HF patients. These are produced to respond to ventricular stretch and wall stress. Moreover, BNP leads to increased glomerular filtration rate (GFR), renal blood flow, and myocardial relaxation [18].

In 1981, de Bold et al. observed a rapid and strong response of natriuretic peptides in rats, induced by intravenous injection of atrial myocardial extract. They reported that the heart, through ANP and BNP, can balance fluid and salt [20]. Also, a natriuretic peptide was described with 28 amino acids and diuretic function as well as natriuretic activity from rat and human atrial muscle in 1983 and 1984, respectively. These hormones were designated ANP and α-human atrial natriuretic polypeptide (α-hANP) [21, 22]. In 1988 and 1990, BNP, with 17 aromatic amino acids, was separated from the porcine brain and human atrium, respectively [23, 24]. The BNP gene is located on the 1p chromosome, which is close to the ANP gene [25]. The BNP gene is upregulated by several factors including cardiomyocyte stretch, injury, and hypoxia [26]. ANP is closer to left-atrial pressure and BNP is close to left-ventricular pressure and bulk index, but BNP may be released from atrial tissue and stored with ANP in atrial storage granules [27–29].

BNP and NT-proBNP are increased in patients with left ventricular systolic dysfunction, as well as in valvular heart disease, pulmonary hypertension, ischemic heart disease, and atrial arrhythmia [30]. In 2001, Kazanegra et al. demonstrated that rapid tests of BNP were beneficial in improving the management of HF in 20 patients with New York Heart Association (NYHA) class III-IV HF [11]. Also, evaluations of BNP and NT-proBNP were beneficial in patients with acute dyspnea diagnosis [31]. In 2009, a meta-analysis of 87,474 participants from 40 prospective studies showed a direct correlation between the rate of BNP or NT-proBNP and risk of CVD [32]. ANP can be used as a biomarker, but the main disadvantage of this peptide is issues with analytical stability. As a suggestion, MRproANP with higher biological stability [33] can be used with BNP and NT-proBNP in obese or elderly patients for which the use of BNP or NT-proBNP is less reliable [13]. Due to the importance of detecting BNP and its cleaved hormone, NT-proBNP, in the diagnosis and prognosis of HF, in this study, we specially discuss the role of biosensors, as a novel detection method, for quantification of these biomarkers. We also provide an overview of the commercial enzyme-linked immunosorbent assay (ELISA) kits in comparison with the biosensors.

BNP activated from proBNP

The prohormone of BNP (proBNP) contains 108 amino acids, which can be divided into active and passive fragments. The active and passive fragments comprise 32 amino acids in the C-terminal fragment and 76 amino acids on the N-terminal fragment (NT-proBNP), respectively, when released into the circulation and mediated by enzymes [34]. The ratio of this separation is 1:1, but NT-proBNP has slower clearance from blood, so its level is higher than that of BNP [35]. The

proBNP may be activated by corin and furin biomarkers that exist on the surface of the cells. These cells are capable of processing and solving proBNP, and so the release of proBNP to the blood increases [36, 37]. The concentration of BNP in the venous bloodstream is very low in healthy conditions, and has a half-life of approximately 20 min [38, 39].

Natriuretic peptide receptors

Natriuretic peptides connect to natriuretic peptide receptors (NPR-A, NPR-B, and NPR-C) at the target cell surface. ANP and BNP attache to NPR-A, while CNP attaches to NPR-B. NPR-C, as a clearance receptor, possesses a higher affinity to ANP in comparison with BNP. Thus, it can lead to increased half-life of BNP [40]. These receptors are identified as GC-A, GC-B, and clearance receptor, respectively [41]. Type A and B receptors lead to guanylate cyclase pathway activity through the augmentation of cyclic guanosine monophosphate (cGMP) and inhibition of RAAS and the sympathetic nervous system, while natriuresis, diuresis, and vasodilation are applied [42].

BNP and heart failure

BNP secretion is controlled at the mRNA transcriptional level, and typically requires longer-term synthesis in stimuli, unlike ANP, which is produced in response to atrial stretch by immediate release from storage granules [20, 43]. Since patients with HF have high levels of undigested proBNP, corin and furin may play an important role in HF [44]. Although some physiological events, such as vasodilatation and inhibition of the RAAS, are caused by the active fragment of BNP, the NT-proBNP amount in serum is about six times higher than the BNP amount. This can be explained by the half-life of BNP and NT-proBNP, which is 20 and 120 min, respectively [39, 45]. For the progression of HF, the neurohumoral activity of the RAAS and the sympathetic nervous system are essential [30]. As described above, the RAAS system and the sympathetic nervous system are controlled by type A and B receptors. Due to clearance or degradation or glomerular filtration of NPs, in patients with hypertension and HF, NP activity may be deficient [31]. Neprilysin, or neutral endopeptidase 24.11, which catalyzes NP degradation, is an important target in HF treatments [32]. Several studies have demonstrated that external BNP may decrease the prevalence of HF and can increase survival [23]. On the other hand, it can reduce hypertension by increasing the secretion of sodium from the kidneys and decrease blood volume.

As mentioned above, the diagnostic efficiency of BNP is greater than that of other natriuretic peptides. Therefore, it can be used as a powerful tool for left ventricular systolic and diastolic function screening [46]. BNP is also considerably higher in neonatal congenital heart disease and in pregnant women with severe preeclampsia [47].

BNP detection

Due to post-translation of BNP and NT-proBNP, these proteins play an important role in HF and are considered a gold standard in HF detection. Factors such as gender, age, renal function, and body mass index can affect BNP test results [48]. Several assays have been reported for the detection of BNP, including rapid immunofluorescence and electrochemiluminescence assay [49]. Competitive immunoassay methods using radiolabeled tracers (radioimmunoassays, RIAs) were introduced as the first assay techniques [50]. The differences between multiple peptides in plasma or tissue samples are the basis for competitive immunoassay. However, several related peptides may affect the properties of these tests. A noncompetitive immunoradiometric assay (IRMA) method can solve this problem and improve BNP assay efficiency [51]. This method showed greater specificity toward BNP based on sandwich immune complex measurement [52]. As multiple biomarkers are best representative of diseases, micromosaic immunoassays (μMIAs) have been developed to demonstrate several cardiac biomarkers such as troponin I and C-reactive protein [53]. Commercial kits for BNP can target both pro-BNP and BNP [54]. However, despite the critical role of protein post-translation, it has been noted that some commercial immunoassay kits are incapable of identifying this post-translation. Despite all the benefits, one of the main problems with this assay is that it is time-consuming. Several methods have been used to overcome this problem. Point-of-care (POC) assays as a type of analytical method have been developed for clinical application in laboratory medicine [55]. Biosensors, as analytical methods which are more in accordance with POC aims, thus play an essential role in clinical and environmental monitoring with the combination of biological and physicochemical parameters. Biosensors many advantages in comparison with other laboratory medicine techniques [56]. Chip-based immunoassays and rapid and reduce experimental time up to 15 min, but these methods provide information in real time [57, 58].

Commercial kits for BNP diagnosis

As already discussed, BNP is considered a gold standard biomarker based on ELISA. In this regard, as shown in Table 1, many commercial kits have been developed based on different methods for the detection of BNP in human samples. Table 1 summarizes the data for ELISA kits extracted from several

sites and represents the analysis of data on commercial kits for BNP diagnosis (https://www.biocompare.com.). ELISA is a primary method used extensively for quantification of proteins and antigens. It is capable of detecting targets based on antigen/antibody interaction in the range of nanograms to picograms per milliliter, illustrating the potential of this method [59]. On the other hand, when this method is compared with biosensors, the latter offer the advantage of portability, simplicity of use, lower cost, and no need for sophisticated equipment. Several biosensors have developed for quantification or qualification detection.

Biosensors for BNP detection

In this regard, biosensors play an important role as a high-throughput technique for selective recognition of biomarkers, and can be classified into electrochemical, electrochemiluminescence, fiber-optic, colorimetric, surface plasmon resonance (SPR), lateral flow, and microfluidic sensors [60, 61]. These methods are highly sensitive, low-cost, rapid, and reliable for detecting BNP levels. The data from studies reporting biosensors designed for detection of BNP are summarized in Table 2.

Electrochemical sensors

Electrochemical biosensors play an important role in rapid diagnostics due to their advantages of robustness, easy miniaturization, and excellent limit of detection (LOD). Variations in pH and ionic stability in different types of sensor receptors may be a limitation with this kind of transducer [110, 111]. There are different electrochemical techniques which produce different signals for detection of analytes. These signals generally include the level of current in amperometric technique, potential or charge accumulation in potentiometric technique, media conductivity properties in conductometric technique, electrical impedance in both resistance and reactance, and changes of current as a function of a voltage to a gate electrode in field effect transistor technology. Enzymes, antibodies, and nucleic acids have been applied to enhance the affinity of biosensors to targets [112]. Antibodies, antibody fragments, or antigens have been used in immunosensors to detect biochemical elements such as BNP and NT-proBNP. Matsuura et al. reported an electrochemical enzyme immunoassay system for BNP in a working range of 20–100 ng/L with a LOD of 10 ng/L. Samples were added to acetylcholinesterase (AChE)-labeled Anti BNP and an immunological response was performed. In this work, to increase BNP sensing, AChE determination was used as the most sensitive method based on electrochemical enzyme immunoassay. Chemisorption/electrochemical desorption of thiocholine on a silver electrode was used to control the AChE activation in this electrochemical enzyme immunoassay system. Eventually, the most cost-efficient kit with an acceptable LOD in comparison with commercial kits was developed [62].

Researchers have focused on the use of nanocomposites to increase the sensitivity of immunosensors and improve signal strength. Zhuo et al. designed an NT-proBNP electrochemical immunosensor based on a composite of gold nanostructures and carbon nanotubes [64]. As shown in Fig. 1A, nanostructured gold and carbon nanotube composites were used to immobilize NT-proBNP antibody for detection. In this study, the secondary antibody was labeled with horseradish peroxidase (HRP) and gold nanochains (AuNCs-HRP-Ab_2) to amplify the detection signal. The proposed immunosensor exhibited a linear range from 0.02 to 100 ng/mL, with a LOD of 6 pg/mL.

In another study, gold nanoparticles (AuNPs) were grafted on the surface of a screen-printed carbon electrode (SPCE) through aryl diazonium salt of 4-aminothiophenol (AuNPs-S-Phe-SPCE) followed by immobilization of the BNP antibodies. This biosensor has the ability to detect BNP in human serum samples with a linear range between 0.014 and 15 ng/mL, and a LOD of 4 pg/mL [74].

In another study, polyaniline (PAN) and tin dioxide (SnO_2) were loaded on graphene sheets (GS) for excellent electrical conductivity. Also, in order to improve biocompatibility, AuNPs were attached on GS/SnO_2/PAN (GS/SnO_2/PAN-Au) [67]. Afterwards, BNP molecules were immobilized on this modified electrode followed by blocking via BSA. In this regard, the signal unit was constructed by immobilization of anti-BNP (Ab) on the nanocomposite of N-doped carbon nanotubes (N-CNTs), $ZnCo_2O_4$, ($ZnCo_2O_4$/N-CNTs) (Fig. 1B). This immunosensor demonstrated a linear range from 0.01 pg/mL to 1 ng/mL, with a LOD of 3.4 fg/mL. This design led to improved LOD, sensitivity, and reproducibility, and outstanding stability with excellent selectivity.

In another work by Maeng et al., an electrochemical immunosensor was developed based on an anti-BNP-single-chain variable fragment (Anti BNP-scFv) expressed in *Pichia pastoris* for BNP antigen with an incubation temperature of 20 °C and pH range of 5.0–7.0 [75]. scFv as part of an antibody plays an important role in antibody detection via the antigen-binding fragment encoded by the VH–linker–VL gene construct [113]. In this study, alkaline phosphatase (AP)-labeled anti-BNP was used to catalyze the oxidation of 4-aminophenyl phosphate to 4-aminophenol (4-AP) in the presence of BNP immobilized on the Au electrode. This biosensor exhibited a wide linear detection range from 1 to 10,000 fg/mL, with a LOD of 1 fg/mL.

Similarly, a label-free electrochemical sensor was developed for multiplex diagnosis of a panel of cardiac biomarkers including cardiac troponin-I (cTnI), cardiac troponin-T

Table 1 Summary of commercial kits for BNP detection

Company	Target Detection	Range detection	
Abcam	BNP		Human
	proBNP		Human
LifeSpan BioSciences	NPPB/BNP	24.69–2000 pg/mL	Human
	NPPB/BNP	39.06–2500 pg/mL	Human
	NPPB/BNP	15.63–500 pg/mL	Human
	NPPB/BNP	0.137–33.33 ng/mL	Human
	NPPB/BNP	8.23–6000 pg/mL	Human
	NPPB/BNP	31.25–2000 pg/mL	Human
R & D Systems	BNP	312.00–10,000 pg/mL	Human
antibodies-online	BNP	31.25–2000 pg/mL	Human
	BNP	24.69–2000 pg/mL	Human
	BNP	0.1–1.000 pg/mL	Human, mouse (Murine), rat (*Rattus*)
	BNP	14–1000 pg/mL	Human
	NPPB	15.6–1000 pg/mL	Human
RayBiotech	BNP	14–1000 pg/mL	Human
	Pro-BNP	0.14–100 ng/mL	Human
	BNP	0.1–1000 pg/mL	Human, Mouse, Rat
MyBioSource.com	BNP		Human
Novus Biologicals	BNP	31.25–2000 pg/mL	Human
	BNP	0.312–20 ng/mL	Human
Eagle Bioscience	BNP	200–6400 pmol/L	Human
	BNP	0–640 pmol/L	Human
Biorbyt	BNP		Human, Mouse, Rat
	BNP		Human
Biomatik	BNP	93.75 pg/mL-6000 pg/mL	Human
	BNP	24.69–2000 pg/mL	*Homo sapiens* (Human)
G-Biosciences	BNP	31.25–2000 pg/mL	Human
Biomedica Medizinprodukte GmbH & Co KG	BNP Fragment	200–6400 pmol/l	Human
Thermo Fisher Scientific	NPPB (BNP)		Human
Enzo Life Sciences, Inc.	BNP		Human
Elabscience Biotechnology Inc.	BNP	31.25–2000 pg/mL	Human
ALPCO	Nt-proBNP	200–6400 pmol/L	Human
Nordic BioSite	BNP	31.25–2000 pg/mL	Human
Krishgen Biosystems	BNP32	1–1000 ng/mL	Human
Peninsula Laboratories International, Inc.	BNP32	0–5 ng/mL	Human
	BNP32	0–10 ng/mL	Human
Assay Solution	Nt-proBNP	313–10,000 pg/mL	Human
Abbexa Ltd	Nt-proBNP	62.5–4000 pg/mL	Human
Abnova Corporation	NPPB		Human
	NPPB		Human
Aviva Systems Biology	Natriuretic peptides B	15.6–1000 pg/mL	Human
	Natriuretic peptides B	0.31–20.0 ng/mL	Human
Signalway Antibody LLC	Nt-proBNP	0.312–20 ng/mL	Human
	NPPB	15.6–1000 pg/mL	Human
Creative Diagnostics	NPPB	0.1–1000 pg/mL	Human
	NPPB	100–2000 pg/mL	Human

Table 2 Summary of data from studies on the design of sensors for detection of BNP

Classification	Target	LOD	Linear range	Method of detection	Type of affinity assay	Reference
Electrochemical	BNP	10 ng/L	20–100 ng/L	Linear sweep voltammetry	Reaction of acetylcholinesterase (AChE)-labeled anti-BNP antibody by BNP followed by measuring AChE activity of recovered antibody–enzyme conjugation through process of chemisorption/electrochemical desorption of thiocholine	[62]
	BNP cTnI	0.9 pg/mL	BNP : 1 pg/mL–1 μg/mL cTnI: 1 pg/m–10 ng/mL	DPV	Gold-based screen-printed electrodes/polyethylenimine/reduced graphene oxide films/propargyl acetic acid/azide-terminated aptamers	[63]
	NT-proBNP	6 pg/mL	0.02–100 ng/mL	CV	CNT/Au/Ab_1 and AuNCs/Ab_2/HRP	[64]
	NT-proBNP	10 fg/mL	10 fg/mL–500 ng/mL	EIS	Nanoporous aluminum oxide/printed circuit board chips/Ab	[65]
	BNP	50 pg/mL	50–200 pg/mL	Amperometry	Gold/titanium electrodes/2D polyaniline layer/anti-BNP antibody	[66]
	BNP	3.4 fg/mL	0.01 pg/mL–1 ng/mL	DPV and amperometry	GS/SnO_2/polyaniline-Au and $ZnCo_2O_4$/N-CNTs/Ab	[67]
	BNP	16 pg/mL	0–4000 pg/mL	EIS	CNT thin film/anti-BNP	[68]
	NT-proBNP, CRP	NT-proBNP: 1 ag/mL CRP: 1 fg/mL	1 ag/mL–10 μg/mL 1 fg/mL–100 pg/mL	EIS	Silicon wafer/chrome layer/gold layer/nanoporous alumina/-dithiobis(succinimidyl propionate)/Ab	[69]
	BNP	100 fM	100 fM–1 nM	FET	Reduced graphene oxide (rGO)/platinum nanoparticles (PtNPs)/modified field effect transistor (FET)/Ab	[70]
	NT-pro BNP	31.5 fg/mL	0.1 pg/mL–50 ng/mL	Square-wave voltammetry (SWV)	$CoSnS_x$/Pd/Ab_2 and Fe_3O_4/PPy/Au/Ab_1 on magnetic glassy carbon electrode (GCE) followed by electrocatalytic activity effect of $CoSnS_x$/Pd/Ab for H_2O_2 oxidation	[71]
	BNP	0.56 pg/mL	1–10,000 pg/mL	CV, DPV	Immune complex between methylene blue/BNP aptamer/AuNPs and Fe_3O_4 magnetic nanoparticles/Ab followed by detection with Au electrode/Ab	[72]
	Atrial natriuretic peptides (ANPs), BNPs	ANP: 0.1 nM BNP: 2.89 pM		Quartz crystal microbalance (QCM)	Amino acid cross-linker (Acr-Cys-$NHBn)_2$ -based epitope-mediated molecularly imprinted polymers (EMIPs)/quartz crystal microbalance (QCM) chips containing gold electrode	[73]
	BNP	4 pg/mL	0.014–15 ng/mL	Amperometric immunosensor	SPCE-S-Phe-AuNPs/Ab	[74]
	BNP	1 fg/mL	1–10,000 fg/mL	Amperometry	Oxidation of 4-APP to produce 4-AP by AP-labeled anti-BNP antibody in presence of BNP immobilized on Au electrode	[75]
	cTnI cTnT BNP	1 pg/mL	1 pg/mL–100 ng/mL	EIS	Anti–cardiac biomarkers (TnT, cTnI and BNP)/ZnO/gold electrode	[76]
	NT-proBNP	0.02 ng/mL	0.12–42.9 ng/mL	Amperometric magneto--immunosensor	Competitive reaction of HRP/anti-NT-proBNP with NT-proBNP/MBs on the Au/SPE electrode in presence of free NT-proBNP followed by addition of TMB-H_2O_2	[77]
	cTnI, creatine kinase MB (CK-MB), BNP	cTnI: 1 pg/mL CK-MB: 0.1 ng/mL BNP: 10 pg/mL	cTnI: 1–300 pg/mL CK-MB: 0.1–3 ng/mL BNP: 10–90 pg/mL	Enzyme-linked immunosorbent assay	Si/SiO_2 layer/Ti/Au electrode/In_2O_3 nanoribbon/Ab_1/antigen/biotinylated Ab_2/streptavidin/biotinylated urease	[78]
	BNP	1.03 pg/mL	1–10,000 fg/mL	CV	SPCE/AuNPs/anti-BNP scFv/antigen/HRP-labeled Anti BNP	[79]

Table 2 (continued)

Classification	Target	LOD	Linear range	Method of detection	Type of affinity assay	Reference
	NT-proBNP	3.7 pg/mL	0.01–50 ng/mL	PEC	ITO/SnO_2/NCQDs/Bi_2S_3	[80]
	BNP	0.05 pg/mL	0.1 pg/mL–5 ng/mL	PEC	Inhibition of PEC produced by SiO_2/polydopamine (PDA)/AgNPs/Ab2/antigen/CeO_2-CdS composites/Ab_1	[81]
	NT-pro BNP	0.03 pg/mL	0.1 pg/mL–100 ng/mL	PEC	Enhancement of PEC produced by Bi_2WO_6 nanaoflower/Ag_2S/thioglycolic acid (TGA)/Ab_1/antigen/GO/PDA/Ab_2	[82]
	BNP		0–1000 pg/mL	Extended gate design of electrical double layer (EDL) field effect transistor (FET)	Hand-held biosensor designed by sensor array chip containing gold electrode pairs/Ab	[83]
Optical	NT-proBNP	0.33 fg/mL	0.001–2 pg/mL	ECL	GCE/PAMAM/Ab_1 and Ab_2/Fc-CsNPs	[84]
	NT-proBNP	1.67 pg/mL	5 pg/mL–25 ng/mL	ECL	PEI/Nafion/Ru-based MOF/Ab_2 and GCE/PtNPs/Ab_1	[85]
	NT-proBNP	0.33 pg/mL	0.001–50 ng/mL	ECL	GCE/Ti:BiOBr-Au/Ab	[86]
	NT-proBNP	0.28 pg/mL	0.0005–100.0 ng/mL	ECL	Ab_1-conjugated gold nanoparticle-modified graphene oxide-Ru$(bpy)_3^{2+}$/$Ag_2C_2O_4$ as luminophor and polydopamine (PDA)-coated Fe_3O_4/Ab_2 as quencher	[87]
	BNP	0.01 pg/mL	0.5 pg/mL–100 ng/mL	ECL	ECL-RET between carbon nitride nanosheets (m-CNNS)/Ab_1 as donor and CeO_2@Polydopamine/Ab_2 (CeO_2@PDA/Ab_2) as acceptor	[88]
	BNP, cTnI	BNP: 3.8 pg/mL cTnl: 3.2 pg/mL	BNP: 0.095–9.33 cTnl: 0.104–10.2 ng/mL	ECL	Simultaneous detection of BNP and cTnI using graphitic phase carbon nitride nanosheets (g-C_3N_4)/AuNPs/anti-BNP_2, N-using (aminobutyl)-N-(ethylisoluminol) (ABEI)/AuNPs/anti-$cTnI_2$ and Au electrode modified by anti-$cTnI_1$ and anti-BNP_1 followed by ABEI/O_2 and g-C_3N_4/$S_2O_8^{2-}$ ECL generation	[89]
	BNP	45 fg/mL	0.074–0.56 pg/mL	Fluorescence	FRET between FAM-modified BNP aptamer as the energy donor and graphene oxide (GO) as acceptor	[90]
	cTnI BNP Myoglobin (Myo)	cTnI: 0.009 ng/mL BNP: 0.084 pg/mL Myo: 0.68 ng/mL	cTnI: 0.01–1000 ng/mL BNP: 0.1–10,000 pg/mL Myo: 1–10,000 ng/mL	Fluorescence	Creation of immune complex between porous hydrogel platform from polyethylene glycol diacrylate (PEGDA) and gelatin/Ab and Cy3/Ab followed by fluorescence microscope detection	[91]
	NT-proBNP CK-MB cTnT	NT-proBNP: 70 pg/mL CK-MB: 910 pg/mL cTnT: 7.8 pg/mL	NT-proBNP: 0.1 ng/mL–200 μg/mL CK-MB: 1–2000 ng/mL cTnT: 0.1–5000 pg/mL	Colorimetry	Ab_1/antigen/GNVs-Ab_2-captured allochroic agents	[92]
	PC PS ATIII PLG BNP cTnI MG		PC: 0.5–2.5 μg/mL PS: 1.5–5 μg/mL ATIII: 45–105 μg/mL PLG: 60–120 μg/mL BNP: 0.0001–0.001 μg/mL	FOB associated with fluorometry	Fiber/Ab_1/antigen/AF647-labeled Ab_2	[93]

Table 2 (continued)

Classification	Target	LOD	Linear range	Method of detection	Type of affinity assay	Reference
	CRP		cTnI: 0.0007–0.007 μg/mL MG: 0.07–0.7 μg/mL CRP: 0.7–7 μg/mL			
	NT-proBNP	0.5 ng/mL	0–1.0 ng/mL	FOB associated with resonance spectra changes	Fiber/APTES/SPA/anti-NT-proBNP mAbs	[94]
	BNP	1 nM		SPR	glass plate/gold/PDMS/titanium/gold/BNP/anti-BNP	[95]
	BNP		<10 aM and 60–100 aM	SPR	Gold chip/MUA/BNP aptamer/BNP/AntiBNP/MUA/gold nanotube	[96]
	BNP	28.2 fg/mL	100 fg/mL–10 ng/mL	SPR	MNP-Ab/BNP/AuNPs-Apt nanoconjugates	[97]
	BNP	0.3 pg/mL	1–10,000 pg/mL	SPR	Porphyrin-mediated calix [4]arene-functionalized AuNP composites (Apt/PyP-pSC4-AuNPs)/BNP/Au chip/prolinker-Cr5B/antiBNP	[98]
LFIA	NT-proBNP	116 ng/L	50–35,000 ng/L	Fluorescence	Lamination card containing UCP/anti-human NT-proBNP in which, after the addition of NT-proBNP on the sample pad, an immune complex was formed on the test line	[99]
	NT-proBNP		50–1200 pg mL^{-1}	Fluorescence	Quantum dot-labeled Ab_1/NT-proBNP/Ab_1	[100]
	NT-proBNP		20–8000 pg/mL	Colorimetry and magnetometry	PAA-Fe_3O_4 MNCs/Ab_2/NT-proBNP/Ab_1	[101]
Microfuidic	BNP	15 fg/mL	5 pg/mL–100 ng/mL	SPR	Collection of anti-BNP-AChE by immobilized BNP on film A followed by collection of produced thiocholine on gold film (film B)	[102]
	Myo cTnI CK-MB BNP	Myo: 100 pg/mL cTnI: 250 fg/mL CK-MB: 150 fg/mL BNP: 50 fg/mL		Conductometry	Label-free sensor based on polyaniline (PANI) nanowire/monoclonal antibody	[103]
	BNP	2.37 ± 1.0 pg/mL	0–400 pg/mL and 700–2500 pg/mL	Fluorometry	Increased fluorescence intensity due to immune complex creation between cyanine-labeled signal antibody (Ab_2) and detection antibody (Ab_1)	[104]
	CEA BNP	<5 pM	0.1–1000 pM	Volumetric bar-chart chip	Detection of produced O_2 from H_2O_2 by catalytic activity of platinum nanoparticles (PtNPs)/Ab_2 and chip/Ab_1	[105]
	BNP	100 pg/mL	100 pg/mL–1 ng/mL	FET	Decrease in current using 2-D PANI/anti-BNP antibodies in presence of BNP	[106]
	BNP	0.012 ng/mL	0.05–30 ng/mL	Electrochemical	SPWE/NH_2-G/Thi/AuNPs/anti-BNP	[107]
	CRP, cTnI, NT-proBNP	CRP: 0.30 ng/mL cTnI: 0.51 ng/mL	CRP: 0.36–42.9 ng/mL cTnI: 1.47–50.1 NT-proBNP: 0.86–69.3 ng/mL	Colorimetry	Bead-based sandwich ELISA type using polystyrene (PS) beads/Ab_1 and Ab_2/HRP	[108]

Table 2 (continued)

Classification	Target	LOD	Linear range	Method of detection	Type of affinity assay	Reference
	CRP, NT-proBNP, cTnI, and fibrinogen	NT-proBNP: 0.24 ng/mL CRP: 0.14 mg/L NT-proBNP: 0.832 pg/mL cTnI: 0.394 pg/mL fibrinogen: 20.2 mg/dL	CRP: 0.1–50 mg/L proBNP: 50–10,000 pg/mL cTnI: 1–10,000 pg/mL fibrinogen: 0.1–5 mg/mL	FET	Si/GaN/AlGaN/Au/aptamer	[109]

(cTnT), and BNP in human serum samples [76]. In this work, ZnO nanorods were synthesized based on low-temperature hydrothermal methods and used as a suitable platform for immobilization of antibodies. The high isoelectric point of pH 9.5, fast electron transfer, surface-charge properties, and signal amplification were the reasons for the use of the ZnO nanostructure. After the fabrication of a ZnO-modified Au electrode, dimethyl sulfoxide (DSP) and thiol-based linker molecules were used for functionalization of the electrode surface. Afterwards, antibodies of cTnI or cTnT or BNP were immobilized with the creation of an amide group using the NHS or NH_2 end of linker molecules. Further, the unbound NHS groups were blocked by SuperBlock to clear nonspecific interactions. Electrochemical impedance spectroscopy (EIS) and Mott–Schottky analysis were used in this study [76]. Mott–Schottky analysis is a method for identifying capacitance-voltage, and it can also be used as a technique for the quantification of doping density and thickness [114]. The binding events of Au electrode/ZnO/antibodies toward the targets including their semiconducting properties compared with a metal surface made the surface suitable for Mott–Schottky analysis and facilitated the occurrence of the electrochemical process in the space charge layer (SCL) and Helmholtz or electrical double layer (EDL). The liner range and LOD of the proposed immunosensor for three biomarkers were 1 pg/mL to 100 ng/mL and 1 pg/mL, respectively.

A recyclable amperometric magnetoimmunosensor was developed by de Ávila et al. for sensitive detection of NT-proBNP through an indirect competitive technique [77]. In this work, NT-proBNP was covalently bound to carboxylic-modified magnetic beads (HOOC-MBs) through N-(3-dimethylaminopropyl)-N′-ethylcarbodiimide (EDC) and N-hydroxysulfosuccinimide (sulfo-NHS). The unreacted activated groups in the MBs were blocked with ethanolamine and then incubated for the detection of the antibody. The HRP-anti-NT-proBNP with a fixed amount was competitively connected with the immobilized NT-proBNP in the presence of free NT-proBNP. The MB immune complexes were immobilized on the Au/SPE surface by a neodymium magnet placed under the working electrode surface (Fig. 1C). The biorecognition event was monitored upon addition of 3,3′,5,5′-tetramethylbenzidine (TMB) and H_2O_2, leading to a linear range of 12–42.9 ng/mL and LOD of 0.02 ng/mL.

A label-free photoelectrochemical (PEC) sensor was fabricated by Fan et al. using modification of an indium tin oxide (ITO) electrode by nitrogen-doped carbon quantum dots (NCQDs) and Bi_2S_3 co-sensitized mesoporous SnO_2 microflower (SnO_2/NCQDs/Bi_2S_3) nanocomposite for detection of NT-proBNP [80]. In this study, tin dioxide (SnO_2), an important n-type semiconductor, was used along with bismuth sulfide (Bi_2S_3) because of its good visible-light absorption properties. Detection of NT-proBNP was achieved by inhibition of electrode transfer via the interaction of NT-proBNP

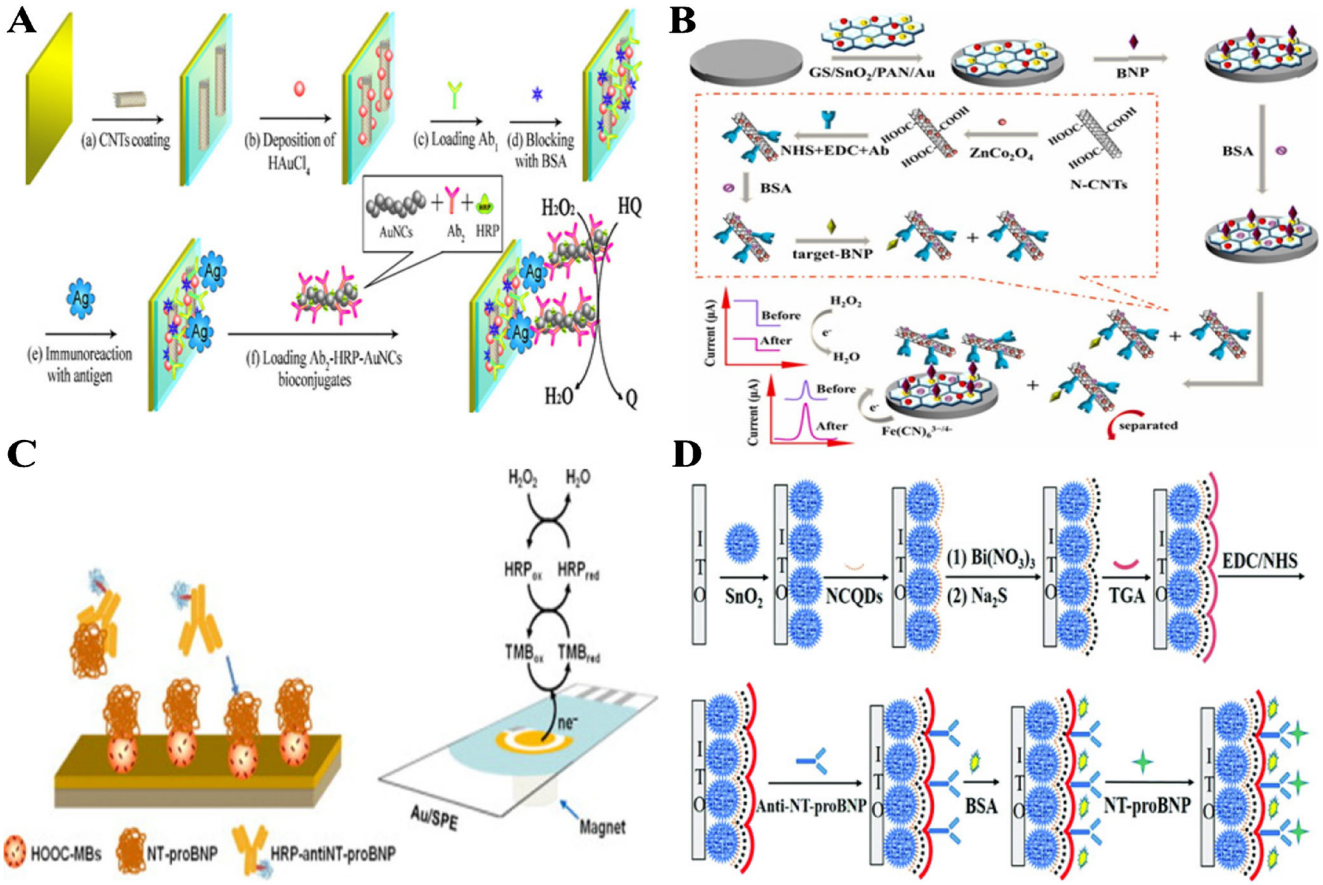

Fig. 1 Schematic illustration of BNP detection by electrochemical sensors: (**A**) AuNCs-HRP-Ab_2 and CNTs-Au-Ab_1. Reprinted from Biosensors and Bioelectronics, Vol 26, Ying Zhuo et al, Ultrasensitive electrochemical strategy for NT-proBNP detection with gold nanochains and horseradish peroxidase complex amplification, p. 2188–2193, Copyright 2011, with permission from Elsevier [64]; (**B**) GS/SnO_2/PAN-Au and $ZnCo_2O_4$/N-CNTs-Ab. Reprinted from Biosensors and Bioelectronics, Vol 126, Xuan Li et al., Dual mode competitive electrochemical immunoassay for B-type natriuretic peptide based on GS/SnO_2/polyaniline-Au and $ZnCo_2O_4$/N-CNTs, p. 448-454, Copyright 2019, with permission from Elsevier [67]; (**C**) HRP/anti-NT-proBNP and NT-proBNP/MBs on the Au/SPE electrode. Reprinted from Analytica Chimica Acta, Vol 784, Berta Esteban-Fernández de Ávila et al., Disposable amperometric magnetoimmunosensor for the sensitive detection of the cardiac biomarker amino-terminal pro-B-type natriuretic peptide in human serum, p. 18-24, Copyright 2013, with permission from Elsevier [77]; (**D**) SnO_2/NCQDs/Bi_2S_3/Ab. Republished with permission of the Royal Society of Chemistry, from [A novel label-free photoelectrochemical immunosensor based on NCQDs and Bi_2S_3 co-sensitized hierarchical mesoporous SnO_2 microflowers for detection of NT-proBNP, Dawei Fan et al., Vol 6, 2018]; permission conveyed through Copyright Clearance Center, Inc.) [80]

and their antibody via electrode transfer inhibition. On the other hand, nitrogen-doped carbon quantum dots (NCQDs) were applied because of their size, low cost, biocompatibility, water solubility, tunable electronic properties, and electron transfer capability. As shown in Fig. 1D, this PEC biosensor layer contained SnO_2/NCQDs/Bi_2S_3, which was prepared using the layer-by-layer synthesis method. The proposed immunosensor exhibited good stability, reproducibility and selectivity toward NT-proBNP, with a linear range of 0.01–50 ng/mL and LOD of 3.7 pg/mL.

Critical note

The review of studies demonstrates that the electrochemical enzyme immunoassays that have been introduced are the most sensitive methods, making it possible to design inexpensive kits in comparison with traditional commercial kits for BNP. A comparison of the data between Table 1 and Table 2 clearly indicates that the LODs of electrochemical sensors are lower than those of commercial kits, which confirms the sensitivity of these electrochemical sensors. Despite their high sensitivity, however, electrochemical sensors are limited by the longer assay time required [62]. The designed electrochemical sensors can be classified into label-free and label-based sensors [115]. The latter contains a recognition unit comprising a capture antibody immobilized (Ab_1) on the modified electrode and a signal probe comprising a detection antibody (Ab_2) on the nanostructure platform which can contain a current enhancer such as a redox agent or enzyme [115]. The former is based on immobilization of the antibody on the electrode

surface followed by binding of the antigen to the antibody, which impedes electron transfer of redox activity [115]. Label-based sensors can also be designed without the need for Ab_1 on the surface of the electrode. The construction of a signal probe for a label-based platform can complicate the sensor design process. Label-based techniques also require signal enhancers such as enzymes, whose activation can be influenced by environment-related conditions. This phenomenon can limit the efficiency of label-based sensors. However, label-free sensors can be constructed using simple, inexpensive, enzyme-free design processes, resulting in a more efficient technique in comparison with label-based sensors. Among electrochemical sensors for BNP, Fan el al. [80] recently introduced a label-free sensor for BNP which must be further developed in the future.

Optical sensors

Electrochemiluminescence

To improve measurement sensitivity, electrochemical detectors can be combined with different transducers such as surface plasmon resonance or optical waveguide lightmode spectroscopy [112]. For the first time, Zhuo et al. introduced a diagnostic system for HF consisting of a signal-off electrochemiluminescence (ECL) immunosensor developed by ferrocene-functionalized chitosan nanoparticles (Fc-CsNPs) as a tag for quenching peroxydisulfate system emission to detect the NT-proBNP [84]. The CsNPs covalently attached to Fc and detected the antibodies (Ab_2/Fc-CsNPs). In this work, a glassy carbon electrode (GCE) was modified with carboxyl polyamidoamine (PAMAM) to enhance the ECL response through immobilization of numerous capture antibodies (Ab_1). According to the fabrication process presented in Fig. 2A, after removal of physically absorbed antibodies via washing with PBS, the NT-proBNP attached to Ab_1 followed by the addition of Ab_2/Fc-CsNPs. The ECL quenching of $S_2O_8^{2-}$ by Fc-CsNPs caused a reduction in the ECL signal, and the concentration of NT-proBNP demonstrated an inverse association with ECL intensity in this study. A wide linear range of 0.001–2 pg/mL and LOD of 0.33 fg/mL were achieved with the application of this biosensor for NT-proBNP.

In addition, a signal-on ECL immunosensor for detection of NT-proBNP in human serum samples was fabricated based on a metal organic framework (MOF) constructed with zinc ions as the central ions and tris(4,4′-dicarboxylicacid2,2′-bipyridyl) ruthenium (II) dichloride $[Ru(dcbpy)3]^{+2}$ as the ligands [85]. The surface of the MOF was modified with nafion and polyethylenimine (PEI) to reduce measurement error during immobilization on a luminophor. Then, the modified MOF (PEI/nafion/MOF) was decorated with AuNPs through Au-N bonds to label the detection antibodies (Ab_2) as a conjugated antibody. In parallel, platinum nanoparticles (PtNPs) were electrodeposited on the GCE followed by immobilization of Ab_1. Finally, a significant enhancement in the ECL signal achieved by the creation of a sandwich immune complex in the presence of NT-proBNP. In this study, $[Ru(dcbpy)^3]^{2+}$ was used because of its excellent ECL activity. Also, Zn^{2+} played an important role in luminescence-functionalized MOF synthesis and coordinated with the six carboxyl groups of $[Ru(dcbpy)^3]^{2+}$. In this fabrication, the functions of PEI and AuNPs were introduced as a coreactant and labeling agent of Ab_2, respectively. Further, AuNPs promoted electron transfer, which enhanced the ECL signal. In particular, the porous structure of MOFs with a large specific area increased the loading of luminophor and coreactant, which further effectively enhanced the ECL response of the proposed immunosensor. The detection range and LOD obtained for the proposed ECL immunosensor were 5–25 ng/mL and 1.67 pg/mL, respectively.

A label-free ECL immunosensor was introduced by Wang et al. based on AuNP-functionalized Ti-doped BiOBr (Ti:BiOBr-Au) to detect NT-proBNP [86]. Bismuth oxybromide (BiOBr) is a novel visible light photocatalyst. Ti was used to recover the ECL feature by increasing the active surface area. AuNPs played a dual role in this ECL via conjugation with antibodies and Ti:BiOBr attachment as well as increased recovery of BiOBr conductivity. Ti:BiOBr-Au was used as the luminophor to construct the sensing platform in this label-free ECL immunosensor. The interaction between NT-proBNP and the antibody led to direct detection via ECL response changes. The linear range and LOD obtained were 0.001–50 ng/mL and 0.33 pg/mL, respectively.

Critical note

ECL sensors possess considerable advantages including high sensitivity and fast response, and thus have been broadly applied for the detection of proteins and nucleic acids. In comparison with fluorescence sensors, ECL sensors do not require an excitation source, thus eliminating autofluorescence or light scattering noise and leading to improved reproducibility and accuracy [116]. Due to the synergistic advantages of electrochemical and luminescence methods, ECL possesses considerable sensitivity, but this method is significantly dependent on the use of expensive redox reagents and expertise, which may limit the development of the ECL method as POC assay. This review indicates that most ECL sensors designed for the detection of BNP are labeled-based sensors, which required covalent binding of Ab_2 on the nanostructures (signal units), increasing the likelihood of inactivation and denaturation of Ab_2 and consequently reduced sensitivity. Therefore, the development of label-free sensors can offer fast, simple, and low-cost analysis of BNP. Among the abovementioned studies for BNP, only Wang et al. [86]

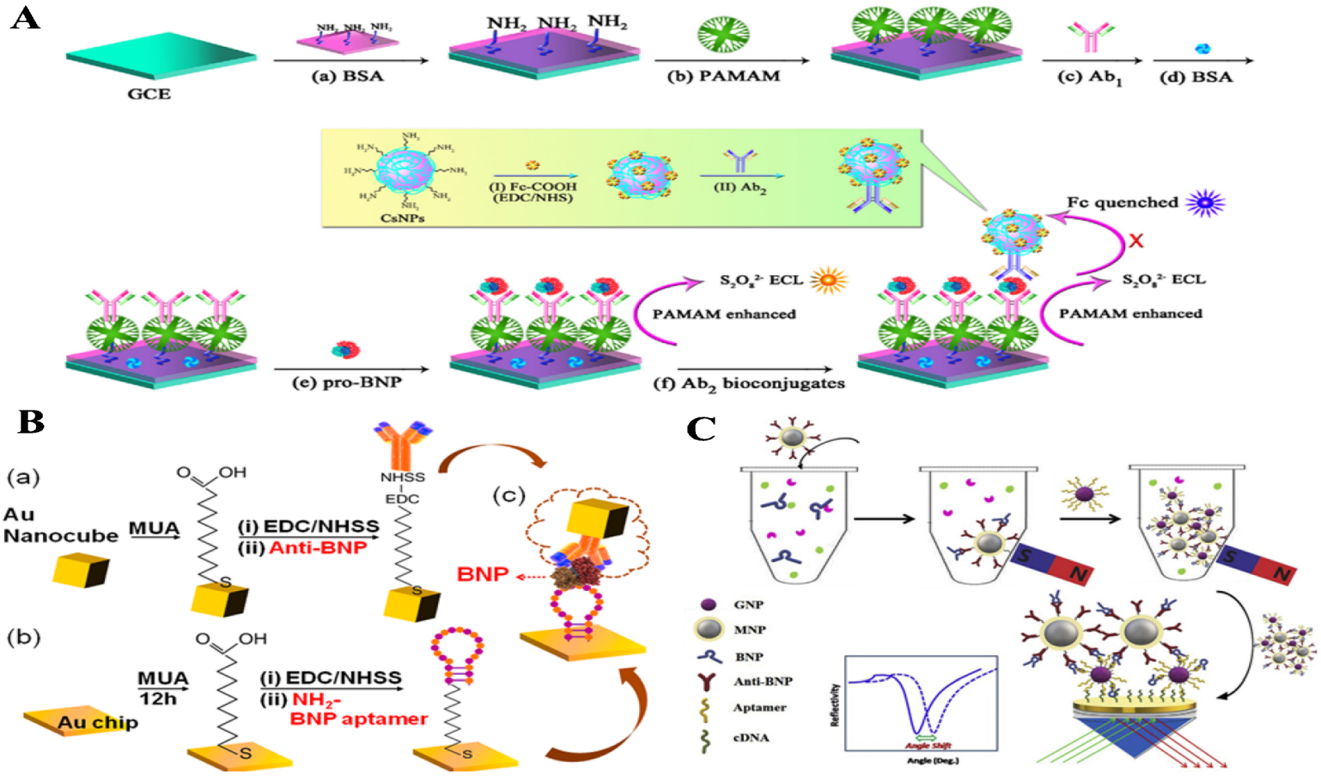

Fig. 2 Schematic illustration of BNP by (**A**) electrochemiluminescence sensors including GCE/PAMAM/Ab_1 and Ab_2/Fc-CsNPs. Reprinted from Sensors and Actuators B: Chemical, Vol 192, Ying Zhuo et al., Quenching of the emission of peroxydisulfate system by ferrocene functionalized chitosan nanoparticles: A sensitive "signal off" electrochemiluminescence immunosensor, p. 791–795, Copyright 2014, with permission from Elsevier [84]; (**B**) SPR sensor using gold chip/MUA/BNP aptamer and AntiBNP/MUA/gold nanocube. Reprinted with permission from [96]. Copyright (2013) American Chemical Society; (**C**) SPR sensor using Fe_3O_4 MNP-Ab and AuNPs-Apt nanoconjugates. Reprinted from Biosensors and Bioelectronics, Vol 141, Jialin Zhao et al., Analyte-resolved magnetoplasmonic nanocomposite to enhance SPR signals and dual recognition strategy for detection of BNP in serum samples, DOI: 10.1016/j.bios.2019.111440, Copyright 2019, with permission from Elsevier [97]

reported a label-free sensor, which must be further developed in future studies.

Fiber-optic sensors

Fiber-optic biosensors (FOB) are used as an important part of optical fields to detect various targets including cells, proteins, and DNA. Tang et al. reported the development of an FOB method to detect CVD biomarkers including anticoagulants (protein C [PC], protein S [PS], antithrombin III [ATIII], and plasminogen [PLG]) and cardiac markers (BNP, cTnI, myoglobin [MG], and CRP) [93]. The sensing unit consisted of four sensors, an automatic flow control unit, and a fluorometer. The fiber surface was coated with streptavidin followed by the addition of Alexa Fluor 647 (AF647) reactive dye-labeled antibody, leading to the creation of an immune complex in the presence of a target.

Similarly, a label-free immunosensor based on excessively tilted fiber gratings (Ex-TFGs) was developed by Luo et al. to detect NT-proBNP [94]. In this study, staphylococcal protein A (SPA), a *Staphylococcus aureus* protein, was used for immobilization of the anti-NT-proBNP monoclonal antibodies (mAbs) on (3-aminopropyl)triethoxysilane (APTES)-modified fiber. The detection of NT-proBNP was processed by changes in the resonance spectra confirmed by a redshift in the resonance peak in the presence of the target. This immunosensor detected NT-proBNP in the range of 0–1.0 ng/mL with LOD of 0.5 ng/mL.

Critical note

In comparison with other biosensors, FOB have gained considerable attention due to their unique properties including easy portability, remarkable sensitivity, easy performance without the need for separation, in vivo, in situ, and real-time detectability, and applicability in whole blood due to a significant reduction in light scattering. This technique can be performed by excitation of fluorophores located in the activation domain of the evanescent wave which is in close proximity to the fiber core (about 100 nm), leading to the elimination of interferences [115]. Also, surface-enhanced Raman spectroscopy (SERS), which is commonly incorporated with the FOB technique, exerts a near-infrared (NIR) window, resulting in reduced autofluorescence and absorption

interference of whole blood in the NIR region [117]. Thus, FOB represents a potent technique for the development and design of new POC assays for clinical use.

Colorimetric sensors

Pu et al. designed an enzyme-free colorimetric immunosensor for determination of acute myocardial infarction (AMI) biomarkers including NT-proBNP, creatine kinase-MB (CK-MB), and cardiac muscle troponin T (cTnT) [92]. This biosensor was constructed based on PH-related encapsulation of three allochroic agents, i.e. phenolphthalein, methyl red, and bromothymol blue, in integrated 3D gold nanovesicles (GNVs). Heat- and PH-triggered release of the allochroic agents from antibody-labeled GNVs led to naked-eye detection of NT-proBNP, CK-MB, and cTnT in the ranges of 0.1 ng/mL to 200 μg/mL (LOD 70 pg/mL), 1–2000 ng/mL (LOD 910 pg/mL), and 0.1–5000 pg/mL(LOD 7.8 pg/mL), respectively.

Critical note

Colorimetric techniques hold a valuable position among different types of biosensors for POC assays of biomarkers due to advantages of visible diagnosis, simplicity, rapid operation, and low cost. Colorimetric methods can be performed in both enzymatic and nonenzymatic forms. The enzymatic method is processed through activation of enzymes in optimal conditions including a specific buffer media and temperature (usually 37 °C) [118]. Therefore, different conditions can influence the efficiency of enzymes. Therefore, the study by Pu et al. [92], which introduced an enzyme-free colorimetric method, is noteworthy.

Surface plasmon resonance (SPR)

SPR methods have been investigated over the past two decades as an important sensor for detecting chemical and biological quantities. For example, Kurita et al. designed an SPR-based immunosensor using a thin polyion complex film containing poly-L-lysine and poly-styrenesulfonate to inhibit nonspecific protein adsorption [95]. To prepare the immunosensor, a glass plate was covered by a thin film of gold, polydimethylsiloxane (PDMS), and titanium, after which the plate was sealed with a polymeric adhesive sheet. Then a solution of poly-L-lysine and poly-styrenesulfonate was added on the surface of the gold film. This SPR immunosensor acted by immobilization of the BNP on the surface. Finally, the interaction of antigen–antibody led to signal changes. The LOD in this biosensor was about 1 nM.

Jang et al. designed an SPR biosensor to detect BNP based on a sandwich assay with a DNA aptamer, a single nucleotide that is used as a monoclonal antibody, and the monoclonal antibody that is modified by gold nanocubes. As shown in Fig. 2B, in this study, the BNP aptamer was immobilized on a gold chip covered by 11-mercaptoundecanoic acid (MUA) and antibody functionalized by gold nanocubes through MUA. The formation of a sandwich immune complex enhanced SPR, leading to detection of BNP in ranges of <10 aM and 60–100 aM [96].

Similarly, Zhao et al. introduced a magnetoplasmonic method using aptamer-functionalized Au nanoparticles (AuNPs-Apt) and antibody-modified Fe_3O_4 magnetoplasmonic nanoparticles (MNPs-Ab) [97]. As shown in Fig. 2C, this method involved the formation of MNP-Ab/BNP/AuNPs-Apt which separated magnetically and dropped onto the cDNA-coated Au chip. This method detected BNP in the range of 100 fg/mL to 10 ng/mL, with LOD of 28.2 fg/mL.

Critical note

The SPR technique can be processed through application of bioreceptor-conjugated nanoparticles suspended in a solution or deposited on a surface followed by incident light on the surface and evaluation of changes in the refractive index (RI) of the surface or redshift of the SPR peak in the presence of a target. Metal nanoparticles, in particular gold nanostructures, are more favorable nanostructures and have been frequently applied in this technique due to the simple functionalization by thiolated molecules and detectability by a UV-Vis spectrophotometer or the naked eye. One issue that should be mentioned is that large antibodies may prevent plasmonic field penetration, preventing molecular detection and decreasing sensitivity [119].

Microfluidic sensors

Microfluidic devices have recently been considered for biomarker detection due to their many benefits, including shorter testing time, less sample usage, and lower chemical and reagent requirements. In this regard, several microfluidic biosensors have been developed to detect targets such as BNP and NT-proBNP. Kurita et al. designed a T-shaped microfluidic device incorporated with a surface plasmon resonance (SPR) sensor for detecting BNP [102]. In this study, antibody-conjugated acetylcholine esterase (AChE) was used as the signal unit. Two gold films (A and B) were coated on the two ports of the microfluidic device. Then, for coating of the BNP on the surface of gold film A, a cystamine monolayer was added, and to enhance this reaction, an EDC/NHS system was applied. Film A detected the unbound anti-BNP-AChE, and film B, with no BNP, determined only the resulting thiocholine concentration due to the attraction of acetylthiocholine by the collected anti-BNP-AChE on film A and monitored by SPR. This microfluidic device showed a dynamic range from 5 pg/mL to 100 ng/mL, with a LOD of

15 fg/mL for trace level measurement of BNP within 30 min in blood samples.

A microfluidic electrochemical sensor was introduced by Zheng et al. using a screen-printed electrode (SPE) to analyze BNP based on a microfluidic paper analytical apparatus and electrochemical immunosensors. For immobilization of the anti-BNP, the SPE was modified with a nanocomposite composed of amino-functional graphene (NH_2-G)/thionine (Thi)/gold nanoparticles (NH_2-G/Thi/AuNPs). The electric flow was produced by the Thi reduction labeled on the surface of the electrode. Also, NH_2-G acted as electric resonance. The electrical flow of the reduction of Thi was reduced due to the creation of an immune complex, leading to the detection of BNP up to 0.012 ng/mL with a linear range of 0.05–30 ng/mL [107].

In another work, a multiplex immunoassay microfluidic sensor was reported by Park et al. for identification of CRP, cTnI, and NT-proBNP based on ELISA [108]. In this lab-on-a-disc, a kind of microfluidic platform, polystyrene (PS) beads were used for immobilization of antibodies. Accordingly, the beads were coated with antibodies in three different chambers followed by the addition of antigens. HRP-conjugated antibodies were then added to detect the targets. This microfluidic biosensor detected biomarkers of CRP, cTnI, and NT-proBNP in linear ranges of 0.36–42.9, 1.47–50.1, and 0.86–69.3 ng/mL, with LODs of 0.30, 0.51, and 0.24 ng/mL, respectively. This sensor was used for diagnosis of biomarkers in whole blood and whole saliva.

Recently, the systematic evolution of ligands by exponential enrichment (SELEX) processes was miniaturized by Sinha et al. on a platform for enrichment aptamers against three major CVD biomarkers, i.e. NT-proBNP, hcTnI, and fibrinogen [120]. In this study, the dissociation constant of aptamers was evaluated by a SPR platform constructed from gold chips decorated by streptavidin followed by conjugation of biotinylated aptamers. In another study, Sinha et al. designed a field-effect transistor (FET) array microfluidic platform based on silicon, gallium nitride (GaN), aluminum-gallium nitride (AlGaN), and Au decorated with aptamers to identify four major CVD protein biomarkers, i.e. CRP, NT-proBNP, cTnI, and fibrinogen [109]. The proposed method successfully detected CRP, NT-proBNP, cTnI, and fibrinogen in ranges of 0.1–50 mg/L (LOD 0.14 mg/L), 50–10,000 pg/mL (LOD 0.832 pg/mL), 1–10,000 pg/mL(LOD 0.394 pg/mL), and 0.1–5 mg/mL (LOD 20.2 mg/dL).

Critical note

Microfluidic techniques have recently garnered significant attention due to their advantages for the development of POC devices, including the low amount of reagent or sample required, fast response, and enhanced sensitivity due to efficient molecular binding and washing [121]. These advantages can facilitate improved clinical processes without the use of unstable and costly materials, and for low amounts and difficult-to-collect samples and reagents. However, the wider use of microfluidic techniques is prevented by disadvantages including difficult preparation of multilayer chips with miniaturized components including chambers, valves, pumps, and channels and the need for expertise, sophisticated technology, and expensive equipment for the connection of chips to a transducer [121].

Lateral flow assay

Lateral-flow immunoassay (LFIA) (also known as immunochromatographic assay or immune-gold colloid immunoassay, IGC) has attracted interested as a method for detection. Benefiting from this method, up-converting phosphor technology-based lateral flow (UCP-LF) was developed by Yang et al. to detect NT-proBNP [99]. In this study, the reporter was constructed by UCP particle-conjugated anti-NT-proBNP. The test and control line strips consisted of anti-human NT-proBNP monoclonal antibody and anti-mouse IgG, respectively. The UPT nanoparticles were NaYF4:Yb^{3+}, Er^{3+}, which were able to be excited at 980 nm and emitted at 541.5 nm. This UPT-LF technique showed a linear range between 50 and 35,000 ng/L and LOD of 116 ng/L.

Similarly, Wilkins et al. demonstrated an LFIA to detect NT-proBNP via a modified monoclonal antibody with quantum dots and showed a linear range of 50–1200 pg/mL [100].

Yang et al. developed an LFIA based on poly(acrylic acid)-stabilized superparamagnetic Fe_3O_4 nanocrystal clusters (PAA-MNCs) as a label for anti-NT-proBNP antibody, to detect NT-proBNP (Fig. 3B) [101]. In this study, magnetic nanocrystal Fe_3O_4 clusters were used to increase the sensitivity of the LFIA sensor. This biosensor was able to detect NT-proBNP qualitatively, with LOD of 100 pg/mL, and quantitatively through the relationship between changes in the magnetic signal and antibody concentration in the range of 20–8000 pg/mL.

Critical note

The lateral flow assay is a simple, inexpensive, and rapid technique which interestingly is in accordance with POC aims but can be limited by some disadvantages. At a high target concentration, the complex target-signal unit (Ab_2-labeled nanoparticles) can pass through the test line and accumulate at the control line, leading to the disappearance of the control line and making detection with the naked eye and device analysis more difficult. AuNPs are the most popular nanoparticles for LFIA and facilitate detection with the naked eye, but may aggregate in whole blood samples. As mentioned in this review, LFIAs for BNP designed using UPT nanoparticles [99],

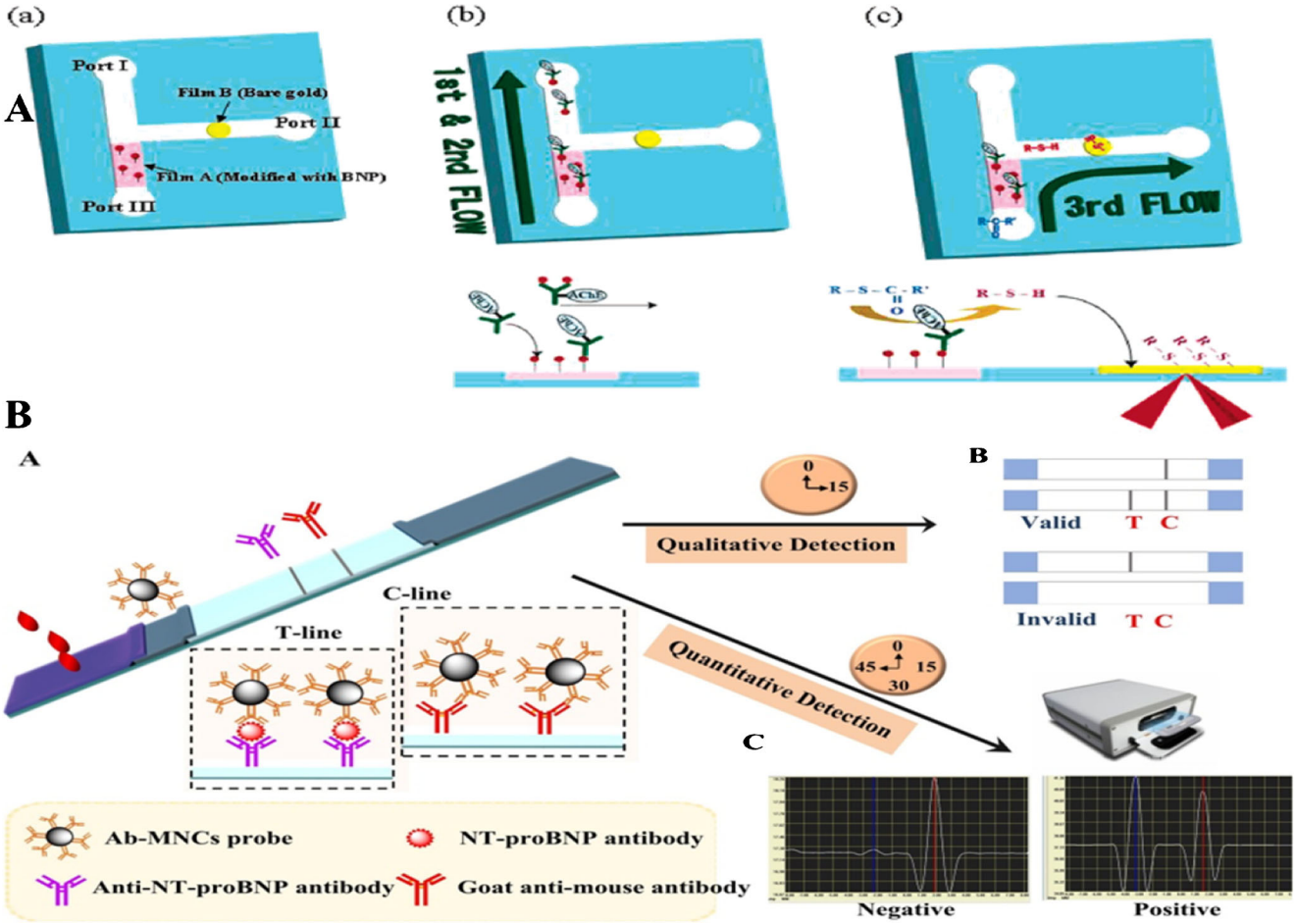

Fig. 3 Schematic illustration of BNP detection by (**A**) microfluidic assay: (a) fabrication of immunosensor: Film A contains immobilized BNP to collect the free anti-BNP-AChE. Film B as a gold film is considered for concentration and detection. (b) Introduction (from port III to port I) of a mixture of BNP and anti-BNP-AChE followed by collection of unreacted anti-BNP-AChE on film A. (c) Introduction of acetylthiocholine from port III to port II followed by production of thiocholine by anti-BNP-AChE and accumulation on film B for SPR detection. Reprinted with permission from [102]. Copyright (2006) American Chemical Society; (**B**) LFIA containing PAA-Fe_3O_4 MNCs/Ab_2. Reprinted from Journal of Pharmaceutical and Biomedical Analysis, Vol 159, Dong Yang et al., One-pot synthesis of poly(acrylic acid)-stabilized Fe_3O_4 nanocrystal clusters for the simultaneously qualitative and quantitative detection of biomarkers in lateral flow immunoassay, p. 119-126, Copyright 2018, with permission from Elsevier [101]

QDs [100], and Fe_3O_4 nanocrystal clusters [101] can resolve these problems with AuNPs.

Conclusion and future perspectives

This review demonstrated that several strategies, including bioconjugation, nanofabrication, and biorecognition, have been successfully employed in the design of platforms for specific detection of BNP. The proposed immunosensors and aptasensors were developed based on combination with enzymes, catalytic nanomaterials, and fluorophores for introduction and application of electrochemical, optical, microfluidic, and LFIA in biological samples. The normal concentration of BNP in blood is less than 7 nM (25 pg/mL), and increases significantly to more than 80 pg/mL [122]. Moreover, clinically, the levels of 100 and 400 pg/mL can predict H to 90% and 95%, respectively [123]. Therefore, the successful measurement at low attomolar ranges suggests that these methods hold promise for clinical use. Moreover, the problem of the low 22-min half-life of BNP can be resolved. The proposed biosensors with advantages of fast response portability, safety, simplicity, and low cost offer a superior alternative to the available commercial immunoassay kits based on isotope or fluorescence detection. Despite these advantages, however, various factors limit the application of the designed biosensors for point-of-care assays of BNP. The colorimetric method is based on the use of AuNPs or other agents which may be affected by the whole blood matrix. In addition specific PH or temperature conditions [92] are necessary for color changes, which can decrease the efficiency of the method due to alterability by environmental conditions. The SPR technique may suffered from low depth of light beam on the surface, leading to lower sensitivity. LFIA

applicability may be affected by a lack of exact distinction between the color of test and control lines, resulting in decreased sensitivity. Electrochemical sensors have generally been fabricated using a label-based design, which is highly dependent on the labeling and use of enzymes [64]. Unfortunately, the labeling process leads to denaturation of biomolecules. Also, the activation of enzymes is strongly affected by environmental conditions. Moreover, ECL method require expensive redox reagents and expertise, which may limit the development of this method as a POC assay. Among different methods, FOB have recently attracted considerable attention, as they avoid the potential biological sample matrix effect. This was made possible by the application of an evanescent wave in close proximity to the fiber core (about 100 nm) which is able to excite the fluorophores on the fiber surface. Incorporation of this technique with SERS, which uses a NIR window, resulted in the reduction of background interference of autofluorescence and absorption related to whole blood. This ability indicates that the FOB technique can be a powerful method for the design of new POC assays. Unfortunately, despite the importance of BNP detection, only a small number of FOB sensors have been introduced, which must be further developed in the future. Most BNP biosensors were immunosensors, which require expensive antibodies that can be unstable under long-term storage conditions. Aptamers with higher affinity and stability in comparison with antibodies can specifically bind to a wide range of targets such as vitamins and viruses and small molecules to macromolecules such as amino acids, peptides, proteins, DNA, and RNA [124, 125]. There, for future studies of BNP detection, aptamers should be applied for the fabrication of sensors.

Acknowledgments The authors gratefully acknowledge the University of Medical Sciences, Mashhad, Iran, for supporting this work.

Declarations

Conflict of interest The authors declare that there are no conflicts of interest regarding this study.

Ethics approval Not applicable.

Source of biological material Not applicable.

Statement on animal welfare Not applicable.

References

1. Alwan A. Global status report on noncommunicable diseases 2010. Geneva: Switzerland World Health Organization; 2011.
2. Mendis S. Cardiovascular risk assessment and management in developing countries. Vasc Health Risk Manag. 2005;1(1):15.
3. Hajifathalian K, Ueda P, Lu Y, Woodward M, Ahmadvand A, Aguilar-Salinas CA, et al. A novel risk score to predict cardiovascular disease risk in national populations (Globorisk): a pooled analysis of prospective cohorts and health examination surveys. Lancet Diabetes Endocrinol. 2015;3(5):339–55.
4. Selvarajah S, Kaur G, Haniff J, Cheong KC, Hiong TG, van der Graaf Y, et al. Comparison of the Framingham risk SCORE, SCORE and WHO/ISH cardiovascular risk prediction models in an Asian population. Int J Cardiol Heart Vasc. 2014;176(1):211–8.
5. D'Aiuto F, Orlandi M, Gunsolley JC. Evidence that periodontal treatment improves biomarkers and CVD outcomes. J Periodontol. 2013;84(4-s):S85–S105.
6. Mozaffarian D, Benjamin EJ, Go AS, Arnett DK, Blaha MJ, Cushman M, et al. American heart association statistics committee and stroke statistics subcommittee. Heart disease and stroke statistics–2015 update: a report from the American Heart Association. Circulation. 2015;131(4):e29–e322.
7. Brouwers FP, Hillege HL, van Gilst WH, van Veldhuisen DJ. Comparing new onset heart failure with reduced ejection fraction and new onset heart failure with preserved ejection fraction: an epidemiologic perspective. Curr Heart Fail Rep. 2012;9(4):363–8.
8. Adebayo SO, Olunuga TO, Durodola A, Ogah OS. Heart failure: definition, classification, and pathophysiology–a mini-review. Nig J Cardiol. 2017;14(1):9.
9. Thomas JT, Kelly RF, Thomas SJ, Stamos TD, Albasha K, Parrillo JE, et al. Utility of history, physical examination, electrocardiogram, and chest radiograph for differentiating normal from decreased systolic function in patients with heart failure. Am J Med. 2002;112(6):437–45.
10. Kannel WB, D ' Agostino RB, Silbershatz H, Belanger AJ, Wilson PW, Levy D. Profile for estimating risk of heart failure. Arch Intern Med. 1999;159(11):1197–204.
11. Kazanegra R, Cheng V, Garcia A, Krishnaswamy P, Gardetto N, Clopton P, et al. A rapid test for B-type natriuretic peptide correlates with falling wedge pressures in patients treated for decompensated heart failure: a pilot study. J Card Fail. 2001;7(1):21–9.
12. Braunwald E. Biomarkers in heart failure. NEJM. 2008;358(20):2148–59.
13. van Kimmenade RR, Januzzi JL. Emerging biomarkers in heart failure. Clin Chem. 2012;58(1):127–38.
14. Sudoh T, Minamino N, Kangawa K, Matsuo H. C-type natriuretic peptide (CNP): a new member of natriuretic peptide family identified in porcine brain. Biochem Biophys Res Commun. 1990;168(2):863–70.
15. MEMBERS NWG, Morrow DA, Cannon CP, Jesse RL, Newby LK, Ravkilde J, et al. National Academy of Clinical Biochemistry Laboratory medicine practice guidelines: clinical characteristics and utilization of biochemical markers in acute coronary syndromes. Circ J. 2007;115(13):e356–e75.
16. Weber M, Hamm C. Role of B-type natriuretic peptide (BNP) and NT-proBNP in clinical routine. Heart J. 2006;92(6):843–9.
17. Burnett J Jr, Granger J, Opgenorth T. Effects of synthetic atrial natriuretic factor on renal function and renin release. Am J Physiol Renal Physiol. 1984;247(5):F863–F6.
18. Cataliotti A, Boerrigter G, Costello-Boerrigter LC, Schirger JA, Tsuruda T, Heublein DM, et al. Brain natriuretic peptide enhances renal actions of furosemide and suppresses furosemide-induced aldosterone activation in experimental heart failure. Circ J. 2004;109(13):1680–5.
19. Mangiafico S, Costello-Boerrigter LC, Andersen IA, Cataliotti A, Burnett JC Jr. Neutral endopeptidase inhibition and the natriuretic peptide system: an evolving strategy in cardiovascular therapeutics. Eur Heart J. 2012;34(12):886–93.

20. de Bold AJ, Bruneau BG. Kuroski de Bold ML. Mechanical and neuroendocrine regulation of the endocrine heart. Cardiovasc Res. 1996;31(1):7–18.
21. Flynn TG, Mercedes L, Adolfo J. The amino acid sequence of an atrial peptide with potent diuretic and natriuretic properties. Biochem Biophys Res Commun. 1983;117(3):859–65.
22. Kangawa K, Matsuo H. Purification and complete amino acid sequence of α-human atrial natriuretic polypeptide (α-hANP). Biochem Biophys Res Commun. 1984;118(1):131–9.
23. Sudoh T, Kangawa K, Minamino N, Matsuo H. A new natriuretic peptide in porcine brain. Nature. 1988;332(6159):78.
24. Kambayashi Y, Nakao K, Mukoyama M, Saito Y, Ogawa Y, Shiono S, et al. Isolation and sequence determination of human brain natriuretic peptide in human atrium. FEBS Lett. 1990;259(2):341–5.
25. Tamura N, Ogawa Y, Yasoda A, Itoh H, Saito Y, Nakao K. Two cardiac natriuretic peptide genes (atrial natriuretic peptide and brain natriuretic peptide) are organized in tandem in the mouse and human genomes. J Mol Cell Cardiol. 1996;28(8):1811–5.
26. van Kimmenade RR, Januzzi JL Jr. The evolution of the natriuretic peptides–current applications in human and animal medicine. J Vet Cardiol. 2009;11:S9–S21.
27. Qi W, Mathisen P, Kjekshus J, Simonsen S, Bjørnerheim R, Endresen K, et al. Natriuretic peptides in patients with aortic stenosis. Am Heart J. 2001;142(4):725–32.
28. Nakao K, Mukoyama M, Hosoda K. Suga S-i, Ogawa Y, Saito Y, et al. biosynthesis, secretion, and receptor selectivity of human brain natriuretic peptide. Can J Physiol Pharmacol. 1991;69(10): 1500–6.
29. Nakamura S, Naruse M, Naruse K, Kawana M, Nishikawa T, Hosoda S, et al. Atrial natriuretic peptide and brain natriuretic peptide coexist in the secretory granules of human cardiac myocytes. Am J Hypertens. 1991;4(11):909–12.
30. Baggish AL, van Kimmenade RR, Januzzi JL Jr. The differential diagnosis of an elevated amino-terminal pro–B-type natriuretic peptide level. Am J Cardiol. 2008;101(3):S43–S8.
31. Kim H-N, Januzzi JL Jr. Natriuretic peptide testing in heart failure. Circ J. 2011;123(18):2015–9.
32. Di Angelantonio E, Chowdhury R, Sarwar N, Ray KK, Gobin R, Saleheen D, et al. B-type natriuretic peptides and cardiovascular risk: systematic review and meta-analysis of 40 prospective studies. Circ J. 2009;120(22):2177–87.
33. Lainscak M, von Haehling S, Anker SD. Natriuretic peptides and other biomarkers in chronic heart failure: from BNP, NT-proBNP, and MR-proANP to routine biochemical markers. Int J Cardiol Heart Vasc. 2009;132(3):303–11.
34. Hama N, Itoh H, Shirakami G, Nakagawa O. Suga S-i, Ogawa Y, et al. rapid ventricular induction of brain natriuretic peptide gene expression in experimental acute myocardial infarction. Circ J. 1995;92(6):1558–64.
35. Bayés-Genís A, Santaló-Bel M, Zapico-Muñiz E, Lopez L, Cotes C, Bellido J, et al. N-terminal probrain natriuretic peptide (NT-proBNP) in the emergency diagnosis and in-hospital monitoring of patients with dyspnoea and ventricular dysfunction. Eur J Heart Fail. 2004;6(3):301–8.
36. Jiang J, Wu S, Wang W, Chen S, Peng J, Zhang X, et al. Ectodomain shedding and autocleavage of the cardiac membrane protease corin. J Biol Chem. 2011:jbc. M110. 185082.
37. Clerico A, Giannoni A, Vittorini S, Passino C. Thirty years of the heart as an endocrine organ: physiological role and clinical utility of cardiac natriuretic hormones. Am J Physiol Heart Circ Physiol. 2011;301(1):H12–20.
38. Holmes S, Espiner E, Richards A, Yandle T, Frampton C. Renal, endocrine, and hemodynamic effects of human brain natriuretic peptide in normal man. J Clin Endocrinol Metab. 1993;76(1):91–6.
39. Mukoyama M, Nakao K, Hosoda K, Suga S, Saito Y, Ogawa Y, et al. Brain natriuretic peptide as a novel cardiac hormone in humans. Evidence for an exquisite dual natriuretic peptide system, atrial natriuretic peptide and brain natriuretic peptide. J Clin Investig. 1991;87(4):1402–12.
40. de Lemos JA, McGuire DK, Drazner MH. B-type natriuretic peptide in cardiovascular disease. Lancet. 2003;362(9380):316–22.
41. Potter LR, Abbey-Hosch S, Dickey DM. Natriuretic peptides, their receptors, and cyclic guanosine monophosphate-dependent signaling functions. Endocr Rev. 2005;27(1):47–72.
42. Boerrigter G, Burnett JC Jr. Recent advances in natriuretic peptides in congestive heart failure. Expert Opin Investig Drugs. 2004;13(6):643–52.
43. Cowie MR, Mendez GF. BNP and congestive heart failure. Prog Cardiovasc Dis. 2002;44(4):293–321.
44. Miyazaki J, Nishizawa H, Kambayashi A, Ito M, Noda Y, Terasawa S, et al. Increased levels of soluble corin in pre-eclampsia and fetal growth restriction. Placenta. 2016;48:20–5.
45. Seino Y, Ogawa A, Yamashita T, Fukushima M. Ogata Ki, Fukumoto H, et al. application of NT-proBNP and BNP measurements in cardiac care: a more discerning marker for the detection and evaluation of heart failure. Eur J Heart Fail. 2004;6(3):295–300.
46. Lee DS, Vasan RS. Novel markers for heart failure diagnosis and prognosis. Curr Opin Cardiol. 2005;20(3):201–10.
47. McDonnell B, Hearty S, Leonard P, O ' Kennedy R. Cardiac biomarkers and the case for point-of-care testing. Clin Biochem. 2009;42(7–8):549–61.
48. Clerico A, Franzini M, Masotti S, Prontera C, Passino C. State of the art of immunoassay methods for B-type natriuretic peptides: an update. Crit Rev Clin Lab Sci. 2015;52(2):56–69.
49. Mayo DD, Colletti JE, Kuo DC. Brain natriuretic peptide (BNP) testing in the emergency department. J Emerg Med. 2006;31(2): 201–10.
50. Dhaliwal AS, Deswal A, Pritchett A, Aguilar D, Kar B, Souchek J, et al. Reduction in BNP levels with treatment of decompensated heart failure and future clinical events. J Card Fail. 2009;15(4): 293–9.
51. Del Ry S, Clerico A, Giannessi D, Andreassi M, Caprioli R, Iascone M, et al. Measurement of brain natriuretic peptide in plasma samples and cardiac tissue extracts by means of an immunoradiometric assay method. Scand J Clin Lab Inv. 2000;60(2):81–90.
52. Yandle T, Richards A, Gilbert A, Fisher S, Holmes S, Espiner E. Assay of brain natriuretic peptide (BNP) in human plasma: evidence for high molecular weight BNP as a major plasma component in heart failure. J Clin Endocrinol Metab. 1993;76(4):832–8.
53. Wolf M, Juncker D, Michel B, Hunziker P, Delamarche E. Simultaneous detection of C-reactive protein and other cardiac markers in human plasma using micromosaic immunoassays and self-regulating microfluidic networks. Biosens Bioelectron. 2004;19(10):1193–202.
54. Clerico A, Zaninotto M, Prontera C, Giovannini S, Ndreu R, Franzini M, et al. State of the art of BNP and NT-proBNP immunoassays: the CardioOrmoCheck study. Clin Chim Acta CLIN CHIM ACTA. 2012;414:112–9.
55. Hawkridge AM, Heublein DM, Bergen HR, Cataliotti A, Burnett JC, Muddiman DC. Quantitative mass spectral evidence for the absence of circulating brain natriuretic peptide (BNP-32) in severe human heart failure. Proc Natl Acad Sci. 2005;102(48):17442–7.
56. Collings A, Caruso F. Biosensors: recent advances. Rep Prog Phys. 1997;60(11):1397.
57. Wang J, Honga B, Kaib J, Hanb J, Zoub Z, Ahnb CH, et al. Mini sensing chip for point-of-care acute myocardial infarction diagnosis utilizing micro-electro-mechanical system and nano-technology. Oxygen Transport to Tissue XXX: Springer; 2009. p. 101–7.

58. Reach G, Wilson GS. Can continuous glucose monitoring be used for the treatment of diabetes. Anal Chem. 1992;64(6):381A–6A.
59. Ma H, Shieh K-J. ELISA Technique. Nat Sci. 2006;4(2):36–7.
60. Leung A, Shankar PM, Mutharasan R. A review of fiber-optic biosensors. Sens Actuators B Chem. 2007;125(2):688–703.
61. Vaddiraju S, Tomazos I, Burgess DJ, Jain FC, Papadimitrakopoulos F. Emerging synergy between nanotechnology and implantable biosensors: a review. Biosens Bioelectron. 2010;25(7):1553–65.
62. Matsuura H, Sato Y, Niwa O, Mizutani F. Electrochemical enzyme immunoassay of a peptide hormone at picomolar levels. Anal Chem. 2005;77(13):4235–40.
63. Grabowska I, Sharma N, Vasilescu A, Iancu M, Badea G, Boukherroub R, et al. Electrochemical aptamer-based biosensors for the detection of cardiac biomarkers. ACS Omega. 2018;3(9): 12010–8.
64. Zhuo Y, Yi W-J, Lian W-B, Yuan R, Chai Y-Q, Chen A, et al. Ultrasensitive electrochemical strategy for NT-proBNP detection with gold nanochains and horseradish peroxidase complex amplification. Biosens Bioelectron. 2011;26(5):2188–93.
65. Selvam AP, Prasad S. Nanosensor electrical immunoassay for quantitative detection of NT-pro brain natriuretic peptide. Futur Cardiol. 2013;9(1):137–47.
66. Liu P, Huang J, Sanchez DVP, Schwartzman D, Lee SH, Yun M. High yield two-dimensional (2-D) polyaniline layer and its application in detection of B-type natriuretic peptide in human serum. Sens Actuators B Chem. 2016;230:184–90.
67. Li X, Liu L, Dong X, Zhao G, Li Y, Miao J, et al. Dual mode competitive electrochemical immunoassay for B-type natriuretic peptide based on GS/SnO 2 /polyaniline-au and ZnCo 2 O 4 /N-CNTs. Biosens Bioelectron. 2019;126:448–54.
68. Li Z, Ausri IR, Zilberman Y, Tang XS. Towards label-free, wash-free and quantitative B-type natriuretic peptide detection for heart failure diagnosis. Nanoscale. 2019;11(39):18347–57.
69. Prasad S, Selvam AP, Reddy RK, Love A. Silicon nanosensor for diagnosis of cardiovascular proteomic markers. J Lab Autom. 2013;18(2):143–51.
70. Lei YM, Xiao MM, Li YT, Xu L, Zhang H, Zhang ZY, et al. Detection of heart failure-related biomarker in whole blood with graphene field effect transistor biosensor. Biosens Bioelectron. 2017;91:1–7.
71. Li Y, Wang Y, Zhang N, Fan D, Liu L, Yan T, et al. Magnetic electrode-based electrochemical immunosensor using amorphous bimetallic sulfides of CoSnS x as signal amplifier for the NT–pro BNP detection. Biosens Bioelectron. 2019;131:250–6.
72. Zhao J, Zhu ZZ, Huang X, Hu X, Chen H. Magnetic gold nanocomposite and aptamer assisted triple recognition electrochemical immunoassay for determination of brain natriuretic peptide. Microchim Acta. 2020;187(4):1–8.
73. Lin CY, Tsai SH, Tai DF. Detection of oxytocin, atrial natriuretic peptide, and brain natriuretic peptide using novel imprinted polymers produced with amphiphilic monomers. J Pept Sci. 2019;25(3):e3150.
74. Serafín V, Torrente-Rodríguez RM, González-Cortés A, García de Frutos P, Sabaté M, Campuzano S, et al. An electrochemical immunosensor for brain natriuretic peptide prepared with screen-printed carbon electrodes nanostructured with gold nanoparticles grafted through aryl diazonium salt chemistry. Talanta. 2018;179: 131–8.
75. Maeng BH, Choi J, Sa YS, Shin JH, Kim YH. Functional expression of recombinant anti-BNP scFv in methylotrophic yeast Pichia pastoris and application as a recognition molecule in electrochemical sensors. World J Microbiol Biotechnol. 2012;28(3):1027–34.
76. Shanmugam NR, Muthukumar S, Tanak AS, Prasad S. Multiplexed electrochemical detection of three cardiac biomarkers cTnI, cTnT and BNP using nanostructured ZnO-sensing platform. Futur Cardiol. 2018;14(2):131–41.
77. de Ávila BE-F, Escamilla-Gómez V, Campuzano S, Pedrero M, Pingarrón JM. Disposable amperometric magnetoimmunosensor for the sensitive detection of the cardiac biomarker amino-terminal pro-B-type natriuretic peptide in human serum. Anal Chim Acta. 2013;784:18–24.
78. Liu Q, Aroonyadet N, Song Y, Wang X, Cao X, Liu Y, et al. Highly sensitive and quick detection of acute myocardial infarction biomarkers using In2O3 nanoribbon biosensors fabricated using shadow masks. ACS Nano. 2016;10(11):10117–25.
79. Shabarni G, Wahyuni HY, Rini S, Toto S. Recombinant anti BNP-SCFV production in *Escherichia coli* and its application for the detection of heart failure by electrochemical immunosensor using Screen-Printed Carbon Electrode-Gold Nanoparticles (SPCE-GNP). Res J Chem Environ. 2018;22(Special issue II):102–7.
80. Fan D, Bao C, Liu X, Wu D, Zhang Y, Wang H, et al. A novel label-free photoelectrochemical immunosensor based on NCQDs and bi2S3 co-sensitized hierarchical mesoporous SnO 2 microflowers for detection of NT-proBNP. J Mater Chem B. 2018;6(46):7634–42.
81. Xu R, Lu P, Wu B, Wang X, Pang X, Du B, et al. Using SiO2/PDA-ag NPs to dual-inhibited photoelectrochemical activity of CeO2-CdS composites fabricated a novel immunosensor for BNP ultrasensitive detection. Sens Actuators B Chem. 2018;274:349–55.
82. Qian Y, Feng J, Fan D, Zhang Y, Kuang X, Wang H, et al. A sandwich-type photoelectrochemical immunosensor for NT-pro BNP detection based on F-bi 2 WO 6 /ag 2 S and GO/PDA for signal amplification. Biosens Bioelectron. 2019;131:299–306.
83. Sarangadharan I, Wang S-L, Tai T-Y, Pulikkathodi AK, Hsu C-P, Chiang H-HK, et al. Risk stratification of heart failure from one drop of blood using hand-held biosensor for BNP detection. Biosens Bioelectron. 2018;107:259–65.
84. Zhuo Y, Han J, Tang L, Liao N, Gui G-F, Chai Y-Q, et al. Quenching of the emission of peroxydisulfate system by ferrocene functionalized chitosan nanoparticles: a sensitive "signal off" electrochemiluminescence immunosensor. Sens Actuators B Chem. 2014;192:791–5.
85. Xiong CY, Wang HJ, Liang WB, Yuan YL, Yuan R, Chai YQ. Luminescence-functionalized metal–organic frameworks based on a ruthenium (II) complex: a signal amplification strategy for Electrogenerated Chemiluminescence Immunosensors. Chem Eur J. 2015;21(27):9825–32.
86. Wang C, Zhu W, Yan T, Yang L, Kuang X, Du B, et al. Novel electrochemiluminescent platform based on gold nanoparticles functionalized Ti doped BiOBr for ultrasensitive immunosensing of NT-proBNP. Sens Actuators B Chem. 2018;277:401–7.
87. Shi L, Li X, Zhu W, Wang Y, Du B, Cao W, et al. Sandwich-type electrochemiluminescence sensor for detection of NT-proBNP by using high efficiency quench strategy of Fe3O4@ PDA toward Ru (bpy) 32+ coordinated with silver oxalate. ACS sensors. 2017;2(12):1774–8.
88. Ali A, Xing B, Khan MS, Ma N, Manzoor R, Wu D, et al. Electrochemiluminescence behaviour of m-CNNS quenched by CeO2@PDA composites for sensitive detection of BNP. J Electroanal Chem. 2020;862:113970.
89. Zhao J, Du J, Luo J, Chen S, Yuan R. A novel potential-resolved electrochemiluminescence immunosensor for the simultaneous determination of brain natriuretic peptide and cardiac troponin I. Sens Actuators B Chem. 2020;311:127934.
90. Tu A, Shang J, Wang Y, Li D, Liu L, Gan Z, et al. Detection of B-type natriuretic peptide by establishing a low-cost and replicable fluorescence resonance energy transfer platform. Microchim Acta. 2020;187(6):1–9.

91. Ji J, Lu W, Zhu Y, Jin H, Yao Y, Zhang H, et al. Porous hydrogel-encapsulated photonic barcodes for multiplex detection of cardiovascular biomarkers. ACS sensors. 2019;4(5):1384–90.
92. Pu Q, Yang X, Guo Y, Dai T, Yang T, Ou X, et al. Simultaneous colorimetric determination of acute myocardial infarction biomarkers by integrating self-assembled 3D gold nanovesicles into a multiple immunosorbent assay. Microchim Acta. 2019;186(3):138.
93. Tang L, Ren Y, Hong B, Kang KA. Fluorophore-mediated, fiber-optic, multi-analyte, immunosensing system for rapid diagnosis and prognosis of cardiovascular diseases. J Biomed Opt. 2006;11(2):021011.
94. Luo B, Wu S, Zhang Z, Zou W, Shi S, Zhao M, et al. Human heart failure biomarker immunosensor based on excessively tilted fiber gratings. Biomed Opt Express. 2017;8(1):57–67.
95. Kurita R, Hirata Y, Yabuki S, Yokota Y, Kato D, Sato Y, et al. Surface modification of thin polyion complex film for surface plasmon resonance immunosensor. Sens Actuators B Chem. 2008;130(1):320–5.
96. Jang HR, Wark AW, Baek SH, Chung BH, Lee HJ. Ultrasensitive and ultrawide range detection of a cardiac biomarker on a surface plasmon resonance platform. Anal Chem. 2014;86(1):814–9.
97. Zhao J, Liang D, Gao S, Hu X, Koh K, Chen H. Analyte-resolved magnetoplasmonic nanocomposite to enhance SPR signals and dual recognition strategy for detection of BNP in serum samples. Biosens Bioelectron. 2019;141.
98. Zhu Z, Li H, Xiang Y, Koh K, Hu X, Chen H. Pyridinium porphyrins and AuNPs mediated bionetworks as SPR signal amplification tags for the ultrasensitive assay of brain natriuretic peptide. Microchim Acta. 2020;187(6):1–9.
99. Yang X, Liu L, Hao Q, Zou D, Zhang X, Zhang L, et al. Development and evaluation of up-converting phosphor technology-based lateral flow assay for quantitative detection of NT-proBNP in blood. PLoS One. 2017;12(2):e0171376.
100. Wilkins MD, Turner BL, Rivera KR, Menegatti S, Daniele M. Quantum dot enabled lateral flow immunoassay for detection of cardiac biomarker NT-proBNP. Sensing and Bio-Sensing Research. 2018;21:46–53.
101. Yang D, Ma J, Xue C, Wang L, Wang X. One-pot synthesis of poly (acrylic acid)-stabilized Fe3O4 nanocrystal clusters for the simultaneously qualitative and quantitative detection of biomarkers in lateral flow immunoassay. J Pharm Biomed Anal. 2018;159:119–26.
102. Kurita R, Yokota Y, Sato Y, Mizutani F, Niwa O. On-chip enzyme immunoassay of a cardiac marker using a microfluidic device combined with a portable surface plasmon resonance system. Anal Chem. 2006;78(15):5525–31.
103. Lee I, Luo X, Huang J, Cui XT, Yun M. Detection of cardiac biomarkers using single polyaniline nanowire-based conductometric biosensors. Biosensors. 2012;2(2):205–20.
104. Fellner S, Hentze S, Kempin U, Richter E, Rocktäschel J, Langer B. Analytical evaluation of a BNP assay on the new point-of-care platform respons®IQ. Pract Lab Med. 2015;2:15–21.
105. Li Y, Xuan J, Song Y, Wang P, Qin L. A microfluidic platform with digital readout and ultra-low detection limit for quantitative point-of-care diagnostics. Lab Chip. 2015;15(16):3300–6.
106. Liu P, Zhu Y, Lee SH, Yun M. Two-dimensional polyaniline nanostructure to the development of microfluidic integrated flexible biosensors for biomarker detection. Biomed Microdevices. 2016;18(6).
107. Zheng Y, Huang Z, Zhang J. Paper-based microfluidic immunoassay for electrochemical detection of B-type natriuretic peptide. Int J Electrochem Sci. 2018;13(7):7246–54.
108. Park J, Sunkara V, Kim T-H, Hwang H, Cho Y-K. Lab-on-a-disc for fully integrated multiplex immunoassays. Anal Chem. 2012;84(5):2133–40.
109. Sinha A, Tai T-Y, Li K-H, Gopinathan P, Chung Y-D, Sarangadharan I, et al. An integrated microfluidic system with field-effect-transistor sensor arrays for detecting multiple cardiovascular biomarkers from clinical samples. Biosens Bioelectron. 2019;129:155–63.
110. D ' Orazio P. Biosensors in clinical chemistry. Clin Chim Acta Clin Chim Acta. 2003;334(1–2):41–69.
111. Wilson MS. Electrochemical immunosensors for the simultaneous detection of two tumor markers. Anal Chem. 2005;77(5):1496–502.
112. Grieshaber D, MacKenzie R, Voeroes J, Reimhult E. Electrochemical biosensors-sensor principles and architectures. Sensors. 2008;8(3):1400–58.
113. Khan FH. Chapter 25 - antibodies and their applications. In: Verma AS, Singh A, editors. Animal biotechnology. San Diego: Academic Press; 2014. p. 473–90.
114. Kirchartz T, Gong W, Hawks SA, Agostinelli T, MacKenzie RC, Yang Y, et al. Sensitivity of the Mott–Schottky analysis in organic solar cells. J Phys Chem C. 2012;116(14):7672–80.
115. Mohammadinejad A, Oskuee RK, Eivazzadeh-Keihan R, Rezayi M, Baradaran B, Maleki A, et al. Development of biosensors for detection of alpha-fetoprotein: as a major biomarker for hepatocellular carcinoma. Trends Anal Chem. 2020;115961.
116. Shen J, Zhou T, Huang R. Recent advances in electrochemiluminescence sensors for pathogenic bacteria detection. Micromachines. 2019;10(8):532.
117. Li X, Zhang Y, Xue B, Kong X, Liu X, Tu L, et al. A SERS nanotag-based fiber-optic strategy for in situ immunoassay in unprocessed whole blood. Biosens Bioelectron. 2017;92:517–22.
118. Yang B, Shi L, Lei J, Li B, Jin Y. Advances in optical assays for detecting telomerase activity. J Lumin. 2019;34(2):136–52.
119. Jonsson MP, Dahlin AB, Jönsson P, Höök F. Nanoplasmonic biosensing with focus on short-range ordered nanoholes in thin metal films. Biointerphases. 2008;3(3):FD30–40.
120. Sinha A, Gopinathan P, Chung Y-D, Lin H-Y, Li K-H, Ma H-P, et al. An integrated microfluidic platform to perform uninterrupted SELEX cycles to screen affinity reagents specific to cardiovascular biomarkers. Biosens Bioelectron. 2018;122:104–12.
121. Chang K-W, Li J, Yang C-H, Shiesh S-C, Lee G-B. An integrated microfluidic system for measurement of glycated hemoglobin levels by using an aptamer–antibody assay on magnetic beads. Biosens Bioelectron. 2015;68:397–403.
122. Mannarino S, Garofoli F, Mongini E, Cerbo RM, Codazzi AC, Tzialla C, et al. BNP concentrations and cardiovascular adaptation in preterm and fullterm newborn infants. Early Hum Dev. 2010;86(5):295–8.
123. Wang P, Jin B, Xing Y, Cheng Z, Ge Y, Zhang H, et al. Rolling circle amplification immunoassay combined with gold nanoparticle aggregates for colorimetric detection of protein. J Nanosci Nanotechnol. 2014;14(8):5662–8.
124. Walsh R, DeRosa MC. Retention of function in the DNA homolog of the RNA dopamine aptamer. Biochem Biophys Res Commun. 2009;388(4):732–5.
125. Rahmati Z, Roushani M, Hosseini H. Three-dimensional NiCo2O4 nanowires encapsulated in nitrogen-doped carbon networks as a high-performance aptamer stabilizer for impedimetric ultrasensitive detection of hepatitis C virus core antigen. Surf Interfaces. 2021;22:100813.